AIP | Applied Physics Letters

(001) textured L10-FePt pseudo spin valve with TiN spacer

P. Ho, G. C. Han, K. H. He, G. M. Chow, and J. S. Chen

Citation: Appl. Phys. Lett. **99**, 252503 (2011); doi: 10.1063/1.3671988
View online: http://dx.doi.org/10.1063/1.3671988
View Table of Contents: http://apl.aip.org/resource/1/APPLAB/v99/i25
Published by the American Institute of Physics.

Related Articles

Anisotropic magnetoresistance in topological insulator Bi1.5Sb0.5Te1.8Se1.2/CoFe heterostructures
AIP Advances 2, 042171 (2012)

Angular-dependences of giant in-plane and interlayer magnetoresistances in Bi2Te3 bulk single crystals
Appl. Phys. Lett. 101, 152107 (2012)

Magnetic field-dependent effective microwave properties of microwire-epoxy composites
Appl. Phys. Lett. 101, 152905 (2012)

Giant magnetoresistance effect in graphene with asymmetrical magnetic superlattices
Appl. Phys. Lett. 101, 152404 (2012)

Giant tunneling magnetoresistance in epitaxial Co2MnSi/MgO/Co2MnSi magnetic tunnel junctions by half-metallicity of Co2MnSi and coherent tunneling
Appl. Phys. Lett. 101, 132418 (2012)

Additional information on Appl. Phys. Lett.

Journal Homepage: http://apl.aip.org/
Journal Information: http://apl.aip.org/about/about_the_journal
Top downloads: http://apl.aip.org/features/most_downloaded
Information for Authors: http://apl.aip.org/authors

ADVERTISEMENT

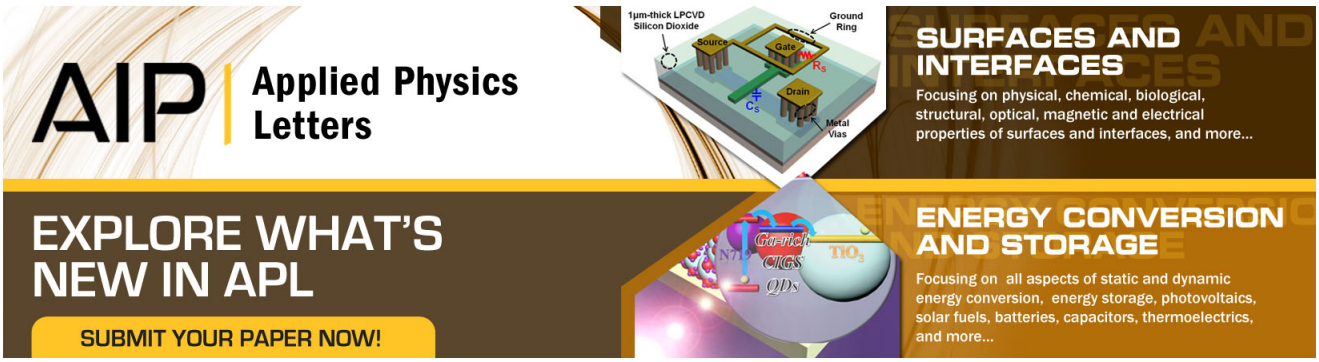

Downloaded 11 Dec 2012 to 137.132.123.69. Redistribution subject to AIP license or copyright; see http://apl.aip.org/about/rights_and_permissions

(001) textured $L1_0$-FePt pseudo spin valve with TiN spacer

P. Ho,[1,2] G. C. Han,[2] K. H. He,[1] G. M. Chow,[1] and J. S. Chen[1,a)]
[1]*Department of Materials Science and Engineering, National University of Singapore, 117576 Singapore*
[2]*Data Storage Institute, Agency of Science, Technology and Research (A*STAR), 117608 Singapore*

(Received 23 October 2011; accepted 5 December 2011; published online 21 December 2011)

TiN was investigated as a potential spacer material in $L1_0$-FePt based pseudo spin valves (PSV). PSVs with the structure MgO/$L1_0$-$Fe_{50}Pt_{50}$ (20 nm)/TiN (5 nm)/$L1_0$-$Fe_{50}Pt_{50}$ (x nm) were fabricated, where x was varied from 5 to 20 nm. The highest giant magnetoresistance (GMR) ratio of 0.61% was obtained for the PSV with a top $L1_0$-FePt thickness of 20 nm. Contributions to the GMR arose from both the spin dependent scattering at the FePt/TiN interfaces and domain wall resistivity. Magnon magnetoresistance was also observed in the fabricated PSVs. © *2011 American Institute of Physics*. [doi:10.1063/1.3671988]

A spin valve consists of a non-magnetic spacer layer sandwiched between two ferromagnets (FM). The FMs switch independently by the deliberate creation of different anisotropy or through the use of an adjacent antiferromagnet to pin the magnetization of the fixed FM. The perpendicular anisotropy spin valve has received much attention as it allows the shrinkage of spintronics devices while ensuring thermal stability with the use of high magnetocrystalline anisotropy (K_u) materials. $L1_0$-FePt is a potential candidate due to its high K_u of 7×10^7 erg/cc.[1] The growth of ordered $L1_0$-FePt involves a high temperature deposition process which will result in interlayer diffusion within the spin valve. Diffusion within the spin valve affects the magnetic, interfacial, and spin transport properties which in turn adversely impacts the magnetoresistance (MR) of the system.[2] The use of a spacer with good diffusion barrier properties and/or the ability to lower the deposition temperature of the adjacent $L1_0$-FePt, while being able to sustain the differential scattering within the spin valve, is very much sought after. Spacer materials such as Ag, Au, and Cu have been used in $L1_0$-FePt based spin valves, but these have been found to diffuse into the FM easily due to the high temperature deposition.[3,4] Recently, epitaxial growth of (001) textured $L1_0$-FePt layer on TiN underlayer has been reported.[5,6] The lattice mismatch of 9.5% between FePt and TiN imposes strain ordering on FePt, thereby promoting the ordered (001) epitaxial relationship. At the same time, the metallic TiN, with low resistivity of 15 $\mu\Omega$ cm, has the desirable qualities of being chemically stable towards FePt and is a good diffusion barrier. This letter introduces the use of TiN as a spacer material in $L1_0$-FePt based pseudo spin valves (PSVs). The morphology of $L1_0$-FePt on TiN is known to be affected by its thickness, and this poses significant changes to the resistance, magnetic, and spin transport properties of the PSVs.[6] In this letter, the magnetic, structural, band structures, and spin transport properties of $L1_0$-FePt/TiN/$L1_0$-FePt PSV with varying thickness of the top $L1_0$-FePt were investigated.

Samples with the structure MgO substrate/$L1_0$-$Fe_{50}Pt_{50}$ (20 nm)/TiN (5 nm)/$L1_0$-$Fe_{50}Pt_{50}$ (x nm) were prepared using magnetron sputtering system with a base pressure better than 8×10^{-7} Torr. The top layer $L1_0$-FePt thickness was varied between 5 to 20 nm. The bottom and top $L1_0$-FePt layers were deposited at 400 and 500 °C, respectively. The TiN spacer layer was deposited at 350 °C. Crystallographic structures were studied using x-ray diffraction (XRD) with Cu K_α radiation. High resolution transmission electron microscopy (HRTEM) was carried out to study the microstructure. Magnetic properties were characterized by the vibrating sample magnetometer (VSM). Current-in-plane (CIP) resistance measurements were made using a four point probe in the presence of a perpendicular-to-plane field. The film nanostructure was determined using the scanning electron microscopy (SEM). First, principles calculations of the band structures of TiN and FePt were performed using the Vienna *ab initio* simulation package (VASP).

The XRD data in Fig. 1 show the FePt (002) fundamental peak and the FePt (001) superlattice peak. In all the PSVs, the chemical ordering parameter (S) resided in a high range of 0.7 to 0.8, indicating the strong presence of (001) $L1_0$ texture in these PSVs (see Table I).[7] No TiN (002) peak was detected as the thin TiN spacer gave rise to a low signal to noise ratio. Fig. 2 shows the HRTEM image of the PSV

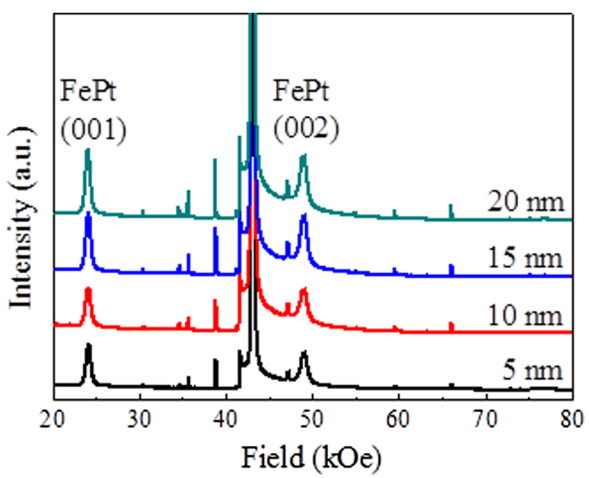

FIG. 1. (Color online) The XRD spectrum of MgO/$L1_0$-FePt/TiN/$L1_0$-FePt PSVs with different top $L1_0$-FePt thicknesses of 5, 10, 15, and 20 nm. The unlabelled sharp peaks are inherent of the MgO substrate.

a)Author to whom correspondence should be addressed. Electronic mail: msecj@nus.edu.sg.

 © 2011 American Institute of Physics

Downloaded 11 Dec 2012 to 137.132.123.69. Redistribution subject to AIP license or copyright; see http://apl.aip.org/about/rights_and_permissions

TABLE I. A summary of the properties of the MgO/$L1_0$-FePt/TiN/$L1_0$-FePt PSVs with the top $L1_0$-FePt of thicknesses 5, 10, 15, and 20 nm.

Thickness (nm)	$S_{001/002}$	$H_{c(hard)}$ (kOe)	$H_{c(soft)}$ (kOe)	$SFD_{(hard)}$ (kOe)	$SFD_{(soft)}$ (kOe)	Resistance (Ω)	GMR (%)
5	0.80	…	3.3	…	0.49	9.22	…
10	0.75	10.1	2.9	4.22	0.44	8.18	0.35
15	0.73	8.5	2.6	3.68	0.44	6.62	0.51
20	0.72	7.6	2.3	2.98	0.44	5.44	0.61

with top $L1_0$-FePt of a thickness of 20 nm. The observation of lattice fringes in the FePt and TiN layers ascertained the growth of (001) textured crystalline FePt and TiN films. A relatively clear and distinct FePt/TiN interface (Fig. 2 inset) also suggested the presence of an effective TiN physical barrier which had minimal reaction with the adjacent FePt layers. In addition, lattice mismatch between TiN and FePt, coupled with the larger TiN elastic modulus, resulted in a slight distortion within the TiN lattice (Fig. 2 inset circle).[8,9]

A single layer of $L1_0$-FePt (20 nm) grown on MgO substrate at 400 °C possessed a coercivity of 1.8 kOe. The hysteresis loops in Fig. 3 show that the top $L1_0$-FePt deposited at 500 °C possessed a larger coercivity than the bottom $L1_0$-FePt, due to the higher deposition temperature which produced a top $L1_0$-FePt with higher K_u. As such, the top harder $L1_0$-FePt assumed the role of a fixed layer while the bottom $L1_0$-FePt the free layer. The difference in coercivity between the top and bottom $L1_0$-FePt as well as the switching field distribution (SFD) of the top $L1_0$-FePt diminished with increasing thickness of top $L1_0$-FePt (Table I). With increasing top $L1_0$-FePt thickness, the $L1_0$-FePt film morphology changed from a particulate island growth to a more complete continuous 3D growth (Fig. 4), resulting in a decrease in its coercivity. Consequently, the difference in coercivity between the top and bottom $L1_0$-FePt reduced. In addition, the increased exchange coupling within the more continuous thicker $L1_0$-FePt film also gave rise to a narrower SFD for the top $L1_0$-FePt. Conversely, for the top $L1_0$-FePt with a thickness of 5 nm, the magnetic moments of the $L1_0$-FePt island-growth grains did not reverse concurrently, contributing to a large SFD [inset of Fig. 3(a)]. Furthermore, a reduction in the resistance of the PSV with increasing thickness of the top $L1_0$-FePt (Table I) was the consequence of a more continuous percolation path for the conduction electrons, which had to pass through the plane of the film during the CIP measurement.

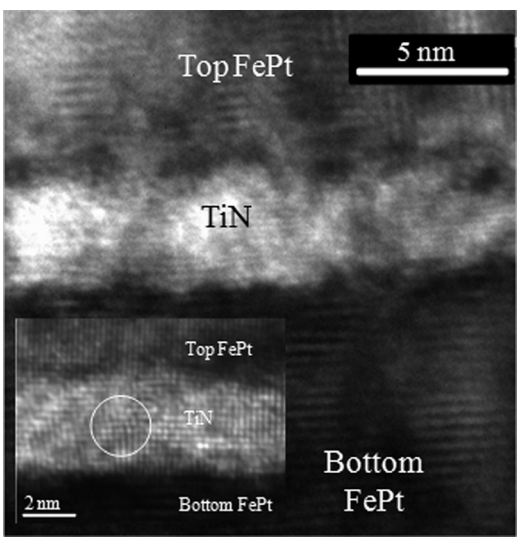

FIG. 2. Cross-sectional HRTEM image showing the epitaxial growth of the bottom $L1_0$-FePt, TiN, and top $L1_0$-FePt films. Inset shows the magnified cross-section of a selected area of the PSV.

A giant magnetoresistance (GMR) of 0.61% was obtained for the PSV with 20 nm of top $L1_0$-FePt [Fig. 3(d)]. The MR hysteresis loop correlated well with the M_s-H hysteresis measurements. An increase in MR occurred when the applied field coincided with the coercivity of the bottom soft $L1_0$-FePt layer, where the PSV was in an anti-parallel configuration. This higher MR was sustained until a field with the same magnitude as the coercivity of the top hard $L1_0$-FePt was applied. The subsequent decline in GMR was attributed to the formation of a parallel configuration within the PSV with the reversal of the top hard $L1_0$-FePt. Fig. 5 shows that near the Fermi energy level of 0 eV, the energy band structures of the FePt spin up electrons displayed better band structure matching with TiN, in terms of more similar energy and slope, compared to that of FePt spin down electrons with TiN.[10] This implied a higher transmission of the majority spin up electrons and a poorer transmission of minority spin down electrons across the $L1_0$-FePt/TiN interface. The $L1_0$-FePt/TiN interfaces acted as spin filters. When the spin filters were aligned (parallel configuration), the majority spin up electrons passed through relatively easily, giving a low resistance state. When the filters were anti-aligned (anti-parallel configuration), the electrons in both channels were reflected at either one of the interfaces, producing a higher resistance state.

At the same time, a spike followed by a sharp dip in MR was observed in the MR loop at the coercive field of the bottom soft $L1_0$-FePt [in Fig. 3(d) labelled (i)]. These sharp changes in resistivity were contributed by the magnon magnetoresistance (MMR) of the bottom free $L1_0$-FePt.[11] This was also observed in a single layer $L1_0$-FePt. At an applied field slightly smaller than the coercive field, the applied field acted in an opposite direction from the magnetization direction. The destabilization of the magnetization direction led to a surge in magnon population, thus bringing about an upsurge in MMR. The magnon population decreased sharply when the applied field and magnetization direction acted in the same direction at the coercive field. Consequently, a reduction in MMR was observed. The MMR was not prominent in the top $L1_0$-FePt possibly due to its larger SFD (Table I). At the coercive field, a considerable number of spins would have reversed, and the remaining spins which contributed to the MMR were significantly reduced.

Downloaded 11 Dec 2012 to 137.132.123.69. Redistribution subject to AIP license or copyright; see http://apl.aip.org/about/rights_and_permissions

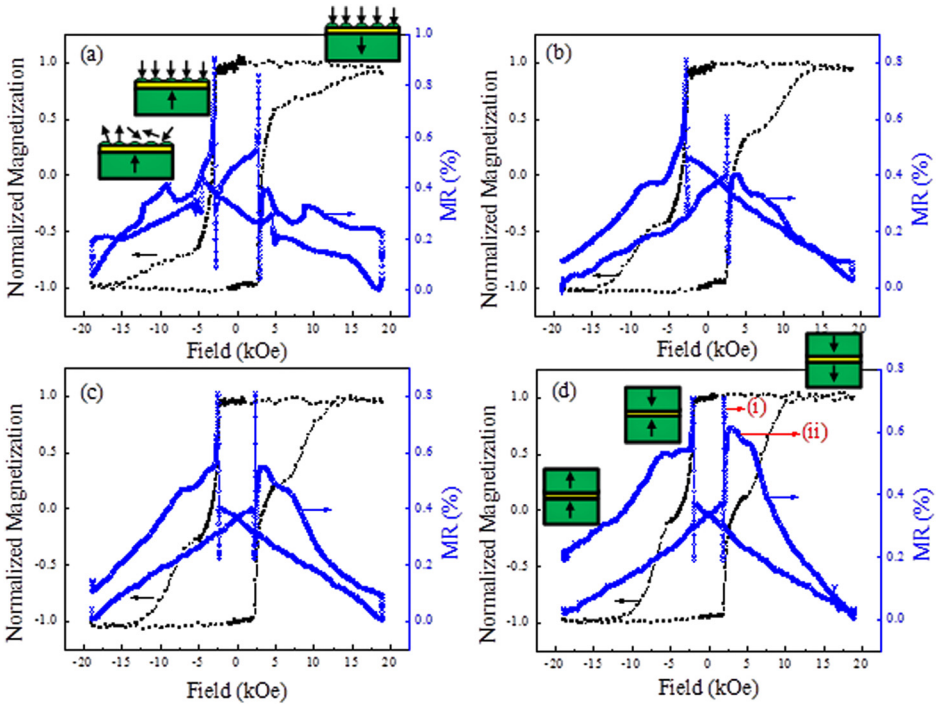

FIG. 3. (Color online) Out-of-plane magnetization (■) and magnetoresistance (x) curves measured at room temperature for MgO/$L1_0$-FePt/TiN/$L1_0$-FePt PSVs with top $L1_0$-FePt thicknesses of (a) 5, (b) 10, (c) 15, and (d) 20 nm.

In addition, a small peak was observed within the region of high GMR where the PSVs assumed an anti-parallel configuration with the reversal of the bottom soft $L1_0$-FePt [in Fig. 3(d) labelled (ii)]. With a high K_u of 4.47×10^7 erg/cc for the bottom $L1_0$-FePt, a narrow domain wall width of 4.7 nm, in the range of the spin diffusion length, was expected. This allowed domain wall scattering by the randomly aligned domains to contribute to GMR during the initial magnetization reversal of the bottom $L1_0$-FePt.[3,12] With an increasing applied field, a saturated state of the bottom $L1_0$-FePt was achieved, and the domain wall resistivity (DWR) diminished, resulting in the disappearance of the peak. Furthermore, it was observed that the MR loop was not saturated at −18 or 18 kOe even though the magnetization loops were well saturated at this field. This was attributed to the finite temperature effect where magnon assisted spin flip *s-d* scattering existed.[13] To achieve saturation of the MR loop, a much larger applied field would be required so as to eliminate this spin disorder.

The GMR of the PSVs decreased with a thinner top $L1_0$-FePt and eventually disappeared with a top $L1_0$-FePt thickness of 5 nm [Fig. 3(a)]. The island growth of the top $L1_0$-FePt prevented a continuous pathway for the spin dependent scattered electrons to be detected via the CIP measurement. Thus, the MR detected in the PSV with 5 nm of top $L1_0$-FePt largely arose from the MMR and DWR contributions. The highest GMR observed was 0.61%, slightly smaller than the use of metallic spacers such as Ag (1.1%) and Pd (0.8%) in (001) textured $L1_0$-FePt based PSVs.[3,14] This was attributed to the larger resistivity of TiN, which led to a greater extent of spin independent scattering, as well as the smaller spin asymmetry of TiN with FePt compared to Ag and Pd. An improvement to the GMR can be achieved with the optimization of the TiN spacer thickness and the insertion of CoFe or

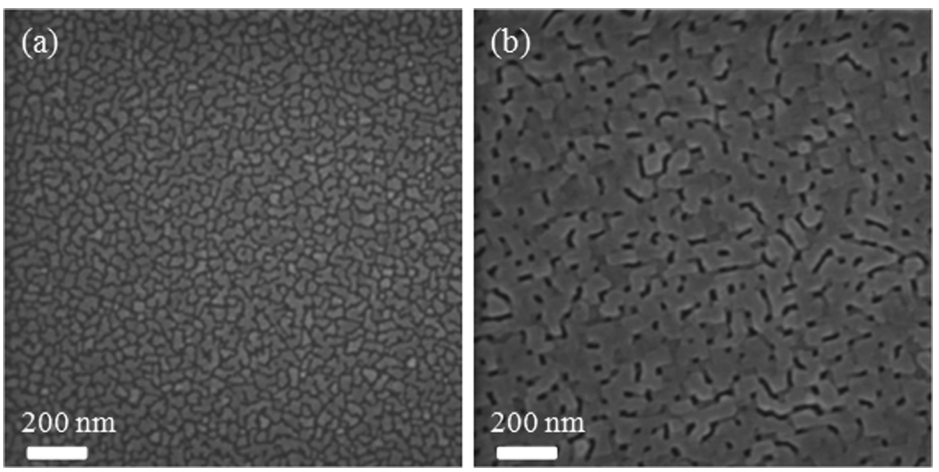

FIG. 4. Plan-view SEM images of top $L1_0$-FePt with thicknesses of (a) 5 and (b) 20 nm for the MgO/$L1_0$-FePt/TiN/$L1_0$-FePt PSVs.

Downloaded 11 Dec 2012 to 137.132.123.69. Redistribution subject to AIP license or copyright; see http://apl.aip.org/about/rights_and_permissions

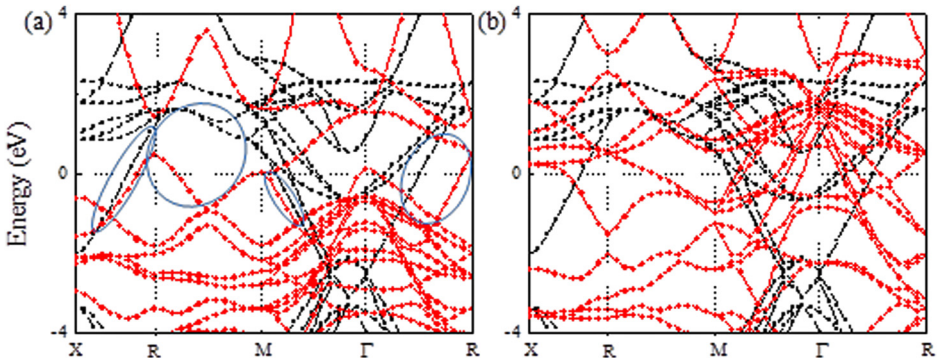

FIG. 5. (Color online) The energy bands for the TiN (■), (a) spin up FePt (●), and (b) spin down FePt (●). Better band match is evident around the Fermi energy of TiN and spin up FePt band structures.

Co spin polarizer layer at the $L1_0$-FePt/TiN interfaces to enhance the interfacial spin polarization.

This work is partially supported by Agency of Science, Technology and Research (A*STAR), Singapore, SERC Grant No. 092-156-0118 and Ministry of Education, Singapore, Tier 1 funding-T11-1001-P04.

[1]T. Seki, S. Mitani, K. Yakushiji, and K. Takanashi, Appl. Phys. Lett. **89**, 172504 (2006).
[2]E. M. Ho, A. K. Petford-Long, and A. Cerezo, J. Magn. Magn. Mater. **192**, 431 (1999).
[3]P. Ho, G. C. Han, R. F. L. Evans, R. W. Chantrell, G. M. Chow, and J. S. Chen, Appl. Phys. Lett. **98**, 132501 (2011).
[4]S. K. Chen, F. T. Yuan, and S. N. Shiao, IEEE Trans. Magn. **41**, 921 (2005).
[5]H. H. Li, K. F. Dong, Y. G. Peng, G. Ju, G. M. Chow, and J. S. Chen, J. Appl. Phys. **110**, 043911 (2011).
[6]Y. Tsuji, S. Noda, and S. Nakamura, J. Vac. Sci. Technol. B **29**, 031801 (2011).
[7]Y. Liu, D. J. Sellmyer, and D. Shindo, *Hand Book of Advanced Magnetic Materials* (Springer, New York, 2006), Vol. **1**, p. 199.
[8]R. O. E. Vijgen and J. H. Dautzenberg, Thin Solid Films **270**, 264 (1995).
[9]P. Rasmussen, X. Rui, and J. E. Shield, Appl. Phys. Lett. **86**, 191915 (2005).
[10]T. Ambrose and O. Mryasov, *Half-Metallic Alloys Fundamentals and Applications*, edited by I. Galanakis and P. H. Dederichs (Springer, Berlin, 2005), pp. 206–210.
[11]A. P. Mihai, J. P. Attané, A. Marty, P. Warin, and Y. Samson, Phys. Rev. B **77**, 060401 (2008).
[12]K. M. Seemann, V. Baltz, M. Mackenzie, J. N. Chapman, B. J. Hickey, and C. H. Marrows, Phys. Rev. B. **76**, 174435 (2007).
[13]J. Yu, U. Rüdiger, A. D. Kent, R. F. C. Farrow, R. F. Marks, D. Weller, L. Folks, and S. S. P. Parkin, J. Appl. Phys. **87**, 6854 (2000).
[14]A. P. Mihai, J. P. Attané, L. Vila, C. Beigné, J. C. Pillet, and A. Marty, Appl. Phys. Lett. **94**, 122509 (2009).

Downloaded 11 Dec 2012 to 137.132.123.69. Redistribution subject to AIP license or copyright; see http://apl.aip.org/about/rights_and_permissions